Mössbauer and crystal-structure study of $YSr_2Cu_2FeO_y$ isomorphic with $YBa_2(Cu_{1-x}Fe_x)_3O_y$

M. Pissas, G. Kallias, A. Simopoulos, D. Niarchos, and A. Kostikas
Institute of Materials Science National Center for Scientific Research "Demokritos," 153 10 Aghia Paraskevi, Attiki, Greece
(Received 1 April 1992)

Mössbauer spectroscopy, magnetic susceptibility, and Rietveld analysis were used to study the magnetic and structural properties of $YSr_2Cu_2FeO_y$ prepared under different annealing conditions. The structure was refined using the tetragonal space group $P4/mmm$ for both the O_2 and the Ar postannealed samples. Mössbauer analysis shows that Fe is equally distributed between the Cu(1) and Cu(2) sites. The hyperfine parameters of Fe in the Cu(2) site are typical of Fe^{3+} in the high-spin state ($S=\frac{5}{2}$) for both samples. The magnetic properties of the system depend strongly on the annealing atmosphere. The O_2 postannealed sample exhibits antiferromagnetic order with $T_N=60$ K, whereas for the Ar postannealed sample $T_N=445$ K.

I. INTRODUCTION

The substitution for Cu with Fe in the $YBa_2(Cu_{1-x}Fe_x)_3O_y$ superconductor is of considerable interest and has been extensively studied with a variety of techniques.[1-6] It is now well established that at a certain Fe doping ($x=0.02-0.03$) and for samples prepared under oxidizing conditions the system undergoes an orthorhombic-to-tetragonal-structural transition and that more oxygen is attracted into the lattice as the Fe content increases.[1,3,6] Moreover, most of the authors agree that for low iron doping ($x<0.1$) the Fe atoms preferentially substitute for Cu at the Cu(1) chain site, whereas for a larger amount of doping there is an increasing tendency to populate the Cu(2) site as well.[1,4,7]

Mössbauer spectroscopy has been proven a powerful tool in the determination of the oxidation state of the substituent Fe atoms as well as their environment (i.e., crystallographic site in the structure). Although it is now apparent that the details of the Mössbauer spectra depend on the thermal history of the sample as well as on oxygen stoichiometry, a considerable amount of experimental evidence appears to be at least qualitatively well established. It is suggested that several different oxygen coordinations exist around the Fe atoms populating the Cu(1) sites (three-, four-, and fivefold) and the valence state of Fe is mainly Fe^{3+} (without however excluding Fe^{2+} and Fe^{4+}).[8-17] The proposed environments are consistent with the results of neutron powder diffraction and EXAFS studies[3,18] that the Fe atom is located primarily at the Cu(1) site, with a small occupation of the Cu(2) site. In particular, there are clearly at least four iron sites which are immediately identifiable by their hyperfine parameters [isomer shift (IS), quadrupole splitting (2ε), and saturation hyperfine field (H)]. Lines and Eibschutz[15] label these sites A (IS=0.28 mm/sec, $2\varepsilon=0.5$ mm/sec), B (IS=0.00 mm/sec, $2\varepsilon=1.19$ mm/sec), C (IS=-0.15 mm/sec, $2\varepsilon=1.61$ mm/sec), and D (IS=0.04 mm/sec, $2\varepsilon=1.94$ mm/sec) in order of increasing room-temperature quadrupole splitting, and it is this labeling we are going to use in this paper.

The study of $YBa_2(Cu_{1-x}Fe_x)_3O_y$ for low iron concentrations is related to the behavior of the Cu(1)-O oxygen deficient layer, since for this doping range Fe substitutes at the Cu(1) site. Our primary interest is focused in the high iron doping region ($x>0.1$), in order to study via Mössbauer spectroscopy the distribution of Fe among the two copper sites, the magnetic behavior of the Cu(2)-O planes as well as the influence of the preparation conditions (i.e., oxygen content) in the magnetic properties of the Cu(2)-O planes.

Recently, Slater *et al.*[19] reported the synthesis of single phase $YSr_2Cu_{3-x}M_xO_y$ for M=Fe, Al, Co, Ga, Pb and for M concentration $0.5<x<1$ with structure identical to that of the $YBa_2Cu_3O_y$ (1:2:3) compound. The metals M showed a strong preference for the Cu(1) site, in complete resemblance with M-substituted 1:2:3. The failure in synthesizing single-phase materials for M=Ni,Zn,Mn—which in the 1:2:3 compound substitute at the Cu(2) site[7,20,21]—as well as single-phase $YSr_2Cu_3O_7$, together with the successful preparation of single-phase materials for M=Fe, Al, Co, Ga, Pb—which in the case of 1:2:3 mainly substitute at the Cu(1) site—led the authors to conclude that the structure is stabilized because of the preferential substitution of these M cations at the Cu(1) site.

In this paper we report a complete series of complementary measurements involving Mössbauer, x-ray diffraction, and dc magnetization studies on $YSr_2Cu_2FeO_y$ samples with thermogravimetrically determined oxygen content. This was done in order to study the distribution of iron in Cu(1) and Cu(2) sites as well as the valence and magnetic properties of the iron as a function of the oxygen content.

II. SAMPLE PREPARATION AND EXPERIMENTAL PROCEDURES

A sample with nominal composition $YSr_2Cu_2FeO_y$ was prepared by thoroughly mixing high purity stoichiometric amounts of Y_2O_3, $SrCO_3$, CuO, and Fe_2O_3. The mixed powders were pelletized and annealed

in air at 980 °C for 24 h and after a second grinding and reformation into pellets the sample was annealed under flowing O_2 at the same temperature for 24 h. Finally, the sample was quenched to room temperature. Two samples were prepared from the as-prepared sample. One after annealing at 600 °C under flowing O_2 [sample (I)] and the other after annealing at 600 °C under flowing Ar [sample (II)]. A subsequent furnace cooling was allowed for both samples in O_2 and Ar atmosphere, correspondingly. The particular temperature of 600 °C was chosen because at this temperature region the kinetics of oxygen intercalation in the 1:2:3 structure are maximized. Finally, we should also mention that annealing of the as-prepared sample at 900 °C under flowing Ar destroyed the Sr phase.

The samples were characterized by x-ray powder diffraction in the Bragg-Brentano geometry with Cu $K\alpha$ radiation using a graphite crystal monochromator (Siemens D500). Mössbauer spectra were taken at 4.2 K, 85 K, and RT using a conventional constant acceleration spectrometer with ^{57}Co(Rh) source moving at RT while the absorber was at the desired temperature. The spectra for temperatures higher than RT were taken in a furnace whose temperature stability was better than 0.2 K. DC magnetization measurements were performed in a SQUID magnetometer (Quantum Design) and thermogravimetric measurements were performed in a TGA apparatus (Perkin Elmer TGS-2) by heating small amounts of the sample under flowing Ar up to 900 °C at a rate of 10 °C/min.

III. THERMOGRAVIMETRY

Figure 1 shows the TGA traces for both samples. As we can see the weight loss of sample (I) is 2.1% and is by far greater than that of sample (II) which is nearly 0.35%. Moreover, sample (I) starts to lose oxygen already at 135 °C whereas sample (II) keeps constant its initial oxygen content up to 600 °C. For sample (I) a change in the slope occurs at 600 °C. We should point out that this inflection point occurs at the same temperature at which sample (II) begins to lose oxygen.

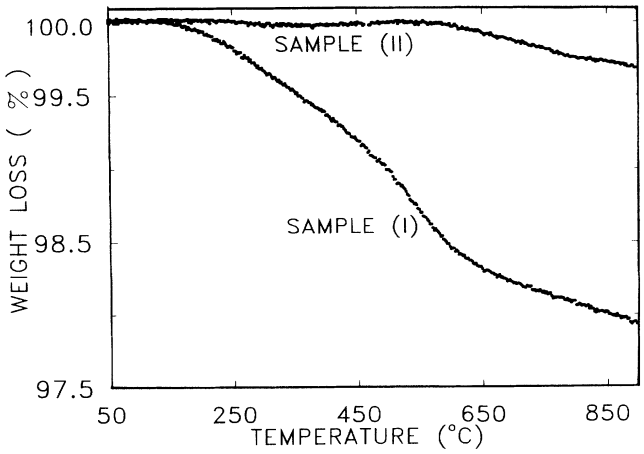

FIG. 1. The TGA traces for samples (I) and (II). The samples were heated under flowing Ar at a rate of 10 °C/min up to 900 °C.

Considering that the initial oxygen content of samples (I) and (II) is $y_i \cong 7.5$ and 6.8, respectively (as determined from the Rietveld profile refinement for these samples) we can deduce from the thermogravimetric curves that the final oxygen content is practically the same—$y_f \cong 6.76$ and 6.65, respectively, for both samples as it would be expected. So, the amount of removable oxygen Δy is about 0.74 oxygen atoms for the oxygen-rich sample and 0.15 for the deoxygenated sample.

IV. STRUCTURAL REFINEMENT

Rietveld profile refinements were done for both samples (I) and (II) in the *P4/mmm* space group. In contrast with Slater *et al.*,[19] we have not introduced any disorder on the oxygen sites O(1) and O(4), considering just the special positions predicted by the *P4/mmm* space group and used in the case of 1:2:3. Furthermore, utilizing the results of our Mössbauer analysis, we have assumed that

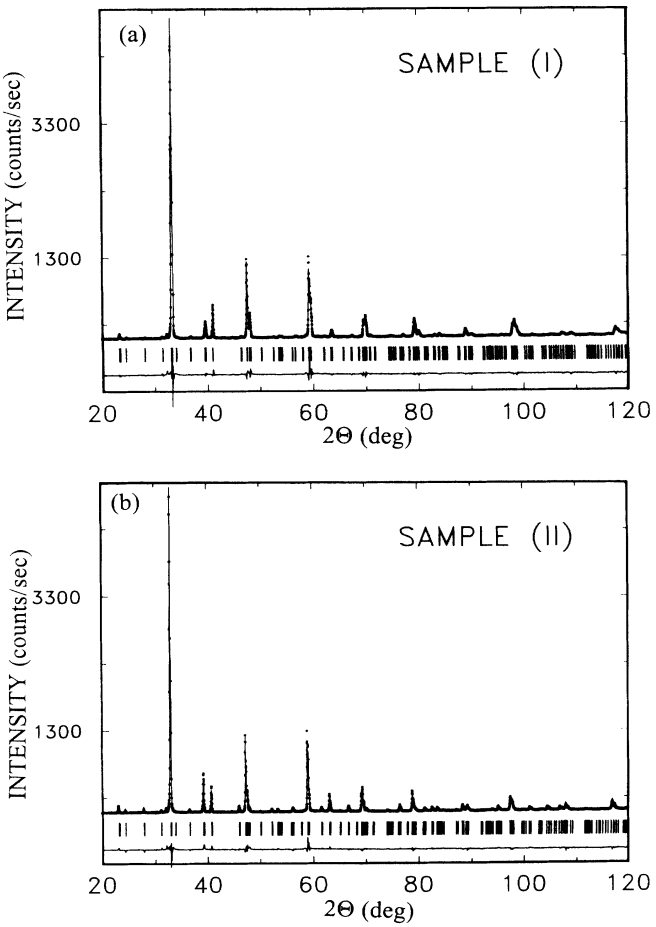

FIG. 2. Rietveld refinement patterns for (a) the oxygen postannealed sample and (b) the Ar postannealed sample. The observed intensities are shown by dots and the calculated ones by the solid line. The positions of the Bragg reflections are shown by the small vertical lines below the pattern. The line in the bottom indicates the intensity difference between the experimental and the refined pattern.

nearly 50% of Fe is located at the Cu(1) site and 50% at the Cu(2) site. Finally, the atomic isotropic temperature factors were kept fixed at the values obtained by Jorgensen *et al.* (see Ref. 23) from neutron powder diffraction studies in 1:2:3 oxygen-rich and oxygen-poor samples.

In Fig. 2 the Rietveld profile refinements of samples (I) and (II) are shown whereas in Fig. 3 an expanded view of the region $38° \leq 2\theta \leq 50°$ is shown. The refined parameters are listed in Table I. In Table I one can see that the oxygen content of sample (I) that was determined by the Rietveld refinement is $y = 7.5 \pm 0.1$, which is in good agreement with the value $y = 7.4 \pm 0.1$ obtained by neutron powder diffraction.[19] In addition, the annealing atmosphere seems to affect considerably the oxygen content of the system since for sample (II) $y = 6.8 \pm 0.1$.

The sensitivity of the oxygen content to the annealing atmosphere is also manifested in the variation of certain structural parameters. The z coordinate of the Sr atom exhibits a large variation from $z = 0.1791$ [sample (I)] to $z = 0.1926$ [sample (II)], in close similarity to what has been reported for the 1:2:3 superconductor as the oxygen content decreases.[22,23] This Sr movement toward the Cu(2)-O planes causes the inversion of the relative intensities of the (014) and (113) reflections (Fig. 3) as well as the considerable increase in the intensity of the (114) reflection which is clearly shown in the diffractogram of sample (II). In addition, the unit cell volume shows a considerable increase as the oxygen decreases and the length of the c axis (which can be taken as a measure of the oxygen content in the 1:2:3 superconductor) presents

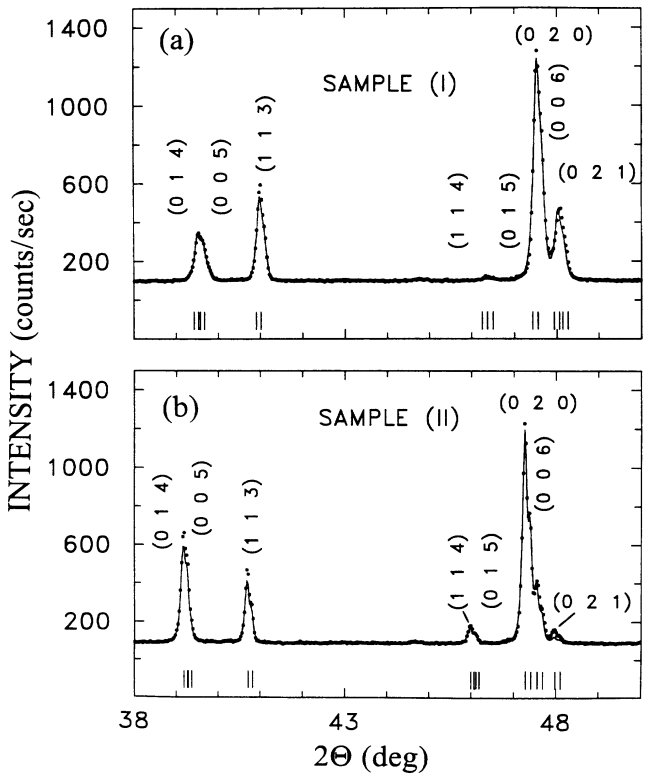

FIG. 3. Rietveld refinement patterns for $YSr_2Cu_2FeO_y$ (a) sample (I) and (b) sample (II) in the region $38° \leq 2\theta \leq 50°$.

TABLE I. Fractional atomic coordinates, isotropic temperature factors, occupancy factors, cell constants, and Rietveld refinement reliability factors for the $YSr_2Cu_2FeO_y$ samples (I) and (II). Rietveld refinements were done in the tetragonal space group $P4/mmm$. The total oxygen content of the samples is defined as $y = 6 + N_{O(1)}$. Atom positions are Y($\frac{1}{2}$ $\frac{1}{2}$ $\frac{1}{2}$), Sr($\frac{1}{2}$ $\frac{1}{2}$ z), Cu(1)(0 0 0), Cu(2)(0 0 z), O(1) (0 $\frac{1}{2}$ 0), O(2)($\frac{1}{2}$ 0 z), and O(4) (0 0 z). The isotropic temperature factors are taken from Ref. 23.

	Sample I	Sample II
a	3.8198(7)	3.8395(7)
c	11.343(1)	11.451(5)
V	165.50	168.80
B_Y	0.28	0.42
z_{Sr}	0.1791(5)	0.1926(5)
B_{Sr}	0.44	0.50
$B_{Cu(1)}$	0.41	0.91
$z_{Cu(2)}$	0.3498(8)	0.3500(7)
$B_{Cu(2)}$	0.20	0.37
$B_{O(1)}$	1.0	0.7
$N_{O(1)}$	1.5±0.1	0.8±0.1
$z_{O(2)}$	0.373(1)	0.374(2)
$B_{O(2)}$	0.4	0.27
$z_{O(4)}$	0.163(4)	0.164(4)
$B_{O(4)}$	0.65	0.61
R_p	7.56	9.91
R_{wp}	7.05	6.97
R_{exp}	1.99	2.12
R_B	5.42	6.22

exactly the same variation with the oxygen content as for 1:2:3, i.e., the higher the oxygen content, the shorter the c axis.[21–23] In contrast, the z coordinate of the apical oxygen O(4) remains nearly constant as the oxygen content varies, in disagreement with the small displacement presented in the case of the 1:2:3 compound. Another interesting point is that the lattice parameter **c** is smaller from that of the 1:2:3 compound, probably due to the fact that Sr has smaller ionic radius than Ba. The insensitivity of the lattice parameter **a** to the Sr substitution probably indicates that the value of **a** is controlled by the Cu(1)-O layers.

V. MÖSSBAUER SPECTRA

Figure 4 shows the Mössbauer spectra of sample (I) at RT and 4.2 K. The parameters obtained from the least-squares fit for both samples are listed in Table II. The RT spectrum of sample (I) was analyzed with two components A and B (according to the labeling of Lines and Eibschutz[15]). The isomer shift of component A (IS=0.265 mm/s, $\varepsilon = 0.290$ mm/s) is typical for Fe^{3+} in the high spin state ($S = \frac{5}{2}$). The main characteristic of the second component B is the low value of the isomer shift (IS$= -0.045$ mm/s).

The 4.2-K spectrum consists of two Zeeman-split components, the first one having hyperfine parameters ($H = 481$ kG, $\varepsilon = -0.134$ mm/s, and IS=0.378 mm/s) which are typical for Fe^{3+} ($S = \frac{5}{2}$). For the quadrupole splitting values of component A at RT and 4.2 K the relation $\varepsilon(LHe) \simeq -(\frac{1}{2})\varepsilon(\mathrm{RT})$ holds, from which we can

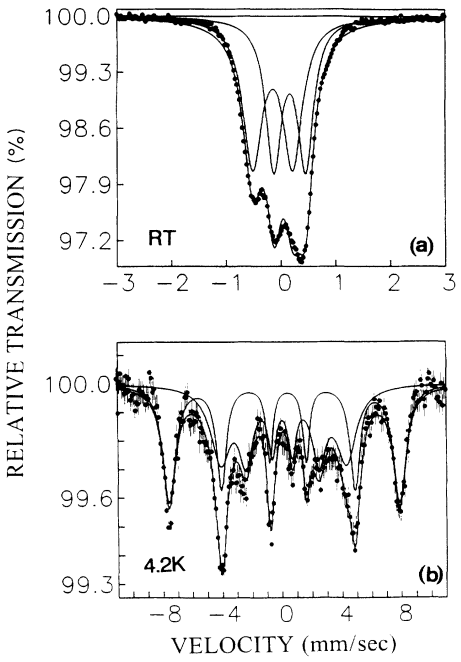

FIG. 4. Mössbauer spectra of $YSr_2Cu_2FeO_y$ [sample (I)] a RT; (b) 4.2 K.

conclude that the magnetic moment of Fe of this component is perpendicular to the z axis of the FEG principal axis system ($\mathbf{s}_{Fe} \perp c$), provided that $\eta \simeq 0$ and $q = V_{zz}/e$ is positive. By examining the value of the isomer shift for this site and comparing it with the values observed for similar compounds[24] and for Fe with distorted square pyramidal environment, we can conclude that this component arises from the iron atoms that occupy the Cu(2) site at which we actually have $\eta \cong 0$ and $V_{zz} \| c$ (as a result of the fourfold symmetry). Therefore the results in the present material are similar to those of the $YBa_2Cu_3O_6$ compound where only the Cu(2) atoms carry magnetic moments that are ordered with the spins laying in the Cu(2)-O planes.[25]

We turn next to discuss the second magnetic component of the 4.2-K spectrum of sample (I). The low value of the magnetic hyperfine field ($H \simeq 263$ kG) together with the small isomer shift (IS=0.089 mm/s), leads us unambiguously to the conclusion that this component cannot be attributed to high spin Fe^{3+} ($S=\frac{5}{2}$). For this component, which is also present in $YBa_2(Cu_{1-x}Fe_x)_3O_y$ it is generally accepted[15] that it originates from Fe which substitutes the Cu(1) site, is fivefold coordinated and its valence state is Fe^{3+} ($S=\frac{3}{2}$).

The discussion of the relative percentages of the various components is based on the assumption that the Debye-Waller factors are equal for the various components. At 4.2 K the relative ratio of the areas of A and B is 46:54 and the same ratio holds for the RT spectrum as well, therefore ensuring the consistency of the assignment. Regarding the distribution of Fe among Cu(1) and Cu(2), we can conclude that component B should arise from Fe at the Cu(1) site (54% of the total Fe content) and component A from Fe at the Cu(2) site (46% of the total Fe content). We should mention however that the neutron powder diffraction results of Slater's work[19] are in disagreement with our Mössbauer results. The reason for this is probably the small difference of the coherent scattering length of Fe and Cu. The determination from the Mössbauer spectra is probably more accurate.

The 458-K spectrum of sample (II) (Fig. 5) consists of two paramagnetic components, component A with IS=0.159 mm/s and ε=0.286 mm/s and component D with IS=0.0067 ms/s and ε=0.765 mm/s. At 445 K

TABLE II. Experimental values of the half-linewidth $\Gamma/2$ in mm/s, the isomer shift IS relative to metallic Fe at RT in mm/s, the quadrupole splitting ε in mm/s ($\varepsilon=(\frac{1}{4})e^2qQ(1+\eta^2/3)^{1/2}$, $\varepsilon=(\frac{1}{8})e^2qQ[3\cos^2\theta-1+\eta\sin^2\theta\cos(2\varphi)]$ for paramagnetic and magnetic spectra, respectively), the hyperfine magnetic field H in kG, the hyperfine magnetic field spread ΔH modulating the line widths, as obtained from least-squares fit of the Mössbauer spectra (the last digit is the significant one).

	Sample	I	II	I	II
	T	RT	458 K	4.2 K	4.2 K
	$\Gamma/2$	0.174	0.288	0.215	0.220
	IS	0.265	0.159	0.378	-0.389
A	ε	0.290	0.286	−0.134	−0.145
	H	0	0	481	508
	ΔH	0	0	16	7
	%	46	48	46	48
	$\Gamma/2$	0.213	0.323	0.252	0.220
	IS	−0.045	0.067	0.089	0.180
B[a]	ε	0.365	0.765	0.03	0.33
	H	0	0	263	350
	ΔH	0	0	32	85
	%	54	52	54	52

[a] B for sample I, D for sample II.

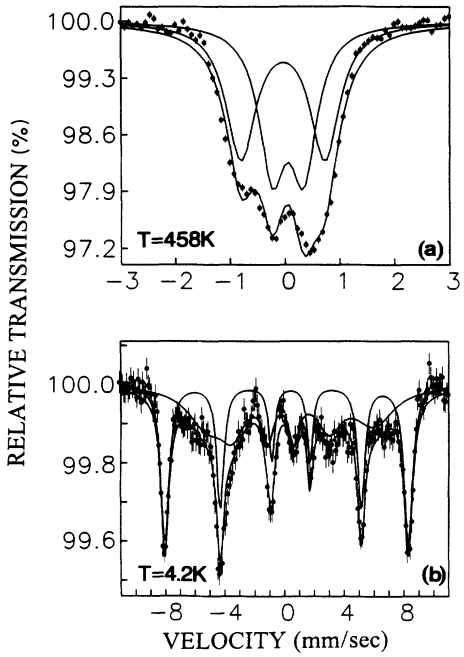

FIG. 5. Mössbauer spectra of $YSr_2Cu_2FeO_y$ [sample (II)] a 458 K, (b) 4.2 K.

component A undergoes a transition from paramagnetic to Zeeman-split Mössbauer spectrum whereas component D remains paramagnetic. The magnetic spectrum of A has been fitted with two magnetic components in order to take into account approximately the distribution of hyperfine fields due to different configurations of nearest-neighbor cations. As temperature decreases and the hyperfine magnetic field reaches the saturation value these components merge into one with a remaining inhomogeneous broadening of the spectral lines.

The 4.2-K spectrum of sample (II) consists of two components, just like the 4.2-K spectrum of sample (I). The first part of the spectrum can be fitted with a sextet whose hyperfine parameters are typical for Fe^{3+} ($S=\frac{5}{2}$) and therefore correspond to the A component of the 445-K spectrum. The second part can be fitted with a sextet that has hyperfine magnetic field $H=350$ kG and IS=0.180 mm/s. Our assignment of this component is that it arises from Fe at the Cu(1) site, which is threefold coordinated and its valence state is Fe^{3+} ($S=\frac{3}{2}$).[15] The broad magnetic hyperfine features [$\Delta H(4.2-K)=85$ kG] which appear at 4.2 K for this component reflect the large degree of disorder of the Cu(1)-O oxygen deficient layer or the existence of intermediate spin relaxation processes.[11,15]

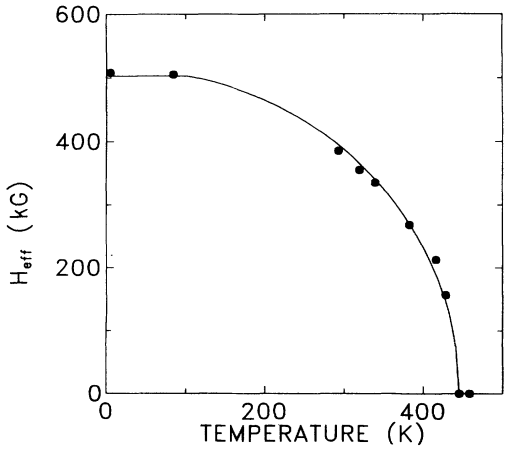

FIG. 6. The variation of the hyperfine field with temperature of Fe in Cu(2) site for sample (II).

Figure 6 shows the variation of the average hyperfine field of the iron in Cu(2) site as a function of temperature, for sample (II). Extrapolating to $H_{hf}=0$ we obtain the transition temperature $T_N=445$ K. The continuous line at the diagram results from the mean-field approximation by solving the equation $\sigma=B_J[(3J)/(J+1)(\sigma/\tau)]$, where $\sigma=H(T)/H(0)$ is the reduced hyperfine field, $\tau=T/T_N$ is the reduced temperature, and J is the spin of Fe in the high spin state ($J=\frac{5}{2}$).

VI. MAGNETIZATION MEASUREMENTS

In order to clarify the magnetic properties of this system, magnetization measurements were also performed for the O_2 postannealed [sample (I)] and for the Ar postannealed sample [sample (II)]. As is shown in Fig. 7 we observed for sample (I) a broad maximum in the susceptibility versus temperature curve near 60 K for magnetic fields smaller than 1 kG. We should also mention that the maximum in the susceptibility curve depends on the external magnetic field. For $H_0=10$ kG the maximum occurs at 40 K. This broad maximum may represent antiferromagnetic long-range order, clustering of the magnetic moments, or even a spin-glass behavior.

The magnetic susceptibility versus temperature data were analyzed using the modified Curie-Weiss type equation $\chi(T)=\chi_0+C/(T-\theta)$ where χ_0 is the temperature

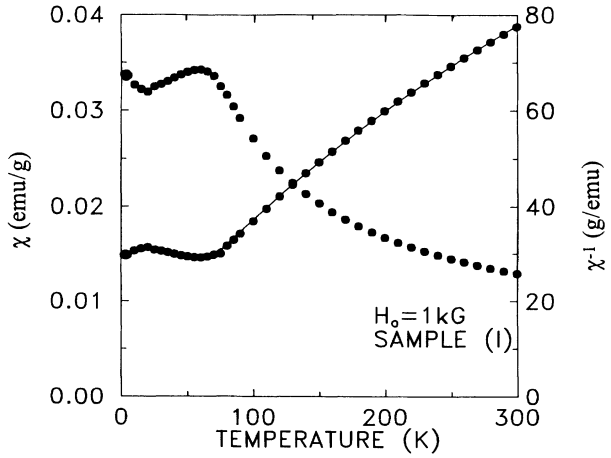

FIG. 7. Temperature dependence of the magnetic susceptibility in $YSr_2Cu_2FeO_y$ for sample (I). The measurement was performed under a magnetic field of 1 kG in the field cooling mode. The solid line represents a least-squares fit of the Curie-Weiss equation (see text).

independent part of the magnetic susceptibility resulting from diamagnetism or Pauli paramagnetism, θ the Weiss constant, and C the Curie constant given by the relation

$$C = N\mu_{\text{eff}}^2\mu_B^2/3k \ ,$$

where N is the number of ions that carry a magnetic moment per unit volume, μ_{eff} the effective number of magnetons per ion, μ_B the Bohr magneton, and k the Boltzmann constant. The parameters χ_0, C, and θ were determined by a least-squares fit for the temperature range 60–300 K. For the data taken with a field $H_0=1$ kG we found that $C=0.015(8)$ deg, $\chi_0=2.3\times10^{-5}$ and $\theta=-25$ K.

Considering that we have three ions per unit cell that carry a magnetic moment then from the C value we extract the effective magnetic moment which is $\mu_{\text{eff}}\cong 2\mu_B$/ion. We should also mention that the μ_{eff} for a sample with the two copper atoms having $S=\frac{1}{2}$, and one iron ion which consists of 50% of the Fe in the $S=\frac{5}{2}$ state and 50% of the Fe in the $S=\frac{3}{2}$ state is equal to 3.21 μ_B/ion. This value differs about $1.2\mu_B$ from the experimental μ_{eff}. This difference can be attributed to the fact that actually the ions have smaller magnetic moments than those presented when considered as free ions, due to covalency effects or more likely to short-range two-dimensional antiferromagnetic interactions at temperature above T_N.

The magnetic susceptibility curve for sample (II) from 4.2 to 360 K (not shown) consists of a paramagnetic part at low T (attributed to the chains) and of a nontemperature-dependent part. We could not go at higher temperatures since the limit of our SQUID is 360 K.

VII. DISCUSSION

In the work of Slater *et al.*,[19] the 86% of the Fe atoms were found to occupy the Cu(1) site with only the remaining 14% located at the Cu(2) site. From the refinements of our x-ray diffractograms we certainly cannot give an answer about the distribution of Fe among the two copper sites, since the x-ray scattering factors of Fe and Cu are very close. However, the analysis of our Mössbauer spectra permits such a determination. In fact, Mössbauer analysis revealed the existence of two components with the relative ratio of their spectral areas being very close to 1 (for the two different preparation conditions studied). At this point, it is worth noticing that annealing under Ar did not result in migration of Fe from the Cu(1) to the Cu(2) site as it was observed in other works.[16]

The A component corresponds to Fe^{3+} ($S=\frac{5}{2}$). From the values of the isomer shift that exist in the literature,[24] we can conclude that the coordination of Fe is certainly less than octahedral, e.g., square pyramidal or tetrahedral. In addition, from the values of the quadrupole splitting in the magnetic as well as in the paramagnetic region, we concluded that the magnetic moment of Fe, in the case of long-range order, is perpendicular to the c axis. This provides additional support for the assignment of this component to Fe in the Cu(2) site since it is known that the Cu(2) site in the $YBa_2Cu_3O_6$ compound has square pyramidal coordination and exhibits similar magnetic properties.

The near 50% Fe occupancy of the square pyramidal Cu(2) site is not surprising since such a coordination of Fe might be rare in the literature but it certainly cannot be ruled out. Recent studies in $Y_2SrCuFeO_y$ (Ref. 26) have pointed out that Fe shares with copper a site with such a coordination. In our work on RBaCuFeO$_{5+x}$,[27] Fe atoms appear in square pyramidal coordination, too.

Comparison with the $YBa_2(Cu_{1-x}Fe_3)O_y$ compound leads us to the conclusion that components B [for sample (I)] and D [for sample (II)] come from iron located at the Cu(1) site. The values of the hyperfine parameter reveal the existence of strong disorder effects with respect to the ligand coordination of iron. Furthermore, the nature of the magnetic spectrum at 4.2 K does not guarantee the existence of long-range order. Most authors[11,15] claim that this magnetic hyperfine structure is due to long paramagnetic spin-relaxation times. Recently, Mirebeau *et al.*[28] studied the $YBa_2(Cu_{0.88}Fe_{0.12})_3O_{6.5}$ compound with neutron diffraction and found that the magnetic structure [alternating antiferromagnetic sheets with similar values of magnetic moment on both Cu(1) and Cu(2) sites] coexists with static and dynamical disorder induced by frustrated Fe spins in the Cu(1) chains, so the magnetic split spectrum at 4.2 K of (B) or (D) coordinate may originate from a long-range order or spins in the slow relaxation limit. Following the arguments of Lines *et al.*[15] both components B and D can be assigned to Fe^{3+} ($S=\frac{3}{2}$) with the former being fivefold coordinated while the latter is threefold coordinated.

As we have already mentioned in the presentation of the Mössbauer results, it is only the hyperfine parameters of component B (and not of component A) that change upon removing oxygen from the system. In particular, the removal of oxygen from the oxygen-rich sample (I) results in increasing the quadrupole splitting of component B (as well as the isomer shift). This behavior can be explained by considering that the coordination number of Fe decreases from V_5 to V_3 (V_n means that the iron ion has n oxygen ligands). Lyubutin *et al.*[17] observed a similar behavior in their Mössbauer study on Fe-doped 1:2:3 as a function of the oxygen content. Therefore, component B has been correctly assigned to the Cu(1)site, since it is well known that the 1:2:3 compound loses oxygen only from the Cu(1)-O oxygen deficient layer. For the same reason the near constancy of hyperfine parameters for component A corroborates the assignment to the Cu(2) site.

The magnetic properties of the Fe atoms that are located at the Cu(2) site were found to be very sensitive to the preparation conditions, that is T_N depends strongly on the oxygen content of the system. In particular, for the oxygen-rich sample $T_N=60\pm5$ K whereas for the deoxygenated sample $T_N=445\pm5$ K. Similar results were observed in the 1:2: 3 compound as well, while it was also found that the Fe concentration had no effect on the T_N.[11] In the $YBa_2Cu_3O_y$ compound the decrease of T_N

with increasing oxygen content has been explained by means of holes that are localized on the oxygen ions.[29] In the undoped 1:2:3 compound for $y < 6.2$, the holes that are created in the chains remain localized within them and so the decrease of the T_N is negligible, while for larger oxygen contents they are transferred to the Cu(2)-O planes resulting in the observed decrease of T_N. Aharony *et al.*[30] have proposed that this effect can be explained by assuming that the hole spin σ interacts via exchange forces with the two neighboring copper spins $\mathbf{s}_1, \mathbf{s}_2$. The Hamiltonians for this interaction is

$$H = -J_\sigma \sigma \cdot (\mathbf{s}_1 + \mathbf{s}_2)$$

and it is intuitively clear that whatever the sign of J_σ, the ground state should correspond to parallel spins $\mathbf{s}_1$ and $\mathbf{s}_2$. This interaction is equivalent to an effective ferromagnetic coupling between $\mathbf{s}_1$ and $\mathbf{s}_2$ of the form $H_{\text{eff}} = -|J_F| \mathbf{S}_1 \cdot \mathbf{S}_2$. The strength of this interaction should be comparable with the antiferromagnetic interaction J producing the antiferromagnetic (AF) order in $YBa_2Cu_3O_6$. The competition between ferromagnetic and antiferromagnetic interactions leads to the frustration of exchange bonding, which results in the destruction of the AF order.

The same mechanism may be operative in the compounds studied in the present work. In our case the Fe ions offer a convenient probe for following the establishment of magnetic order in the Cu(2)-O planes as a function of the hole content.

VII. CONCLUSIONS

In conclusion, we have studied two samples of $YSr_2Cu_2FeO_y$ with different oxygen contents and we have found via Mössbauer spectroscopy that Fe is almost equally distributed among the Cu(1) and Cu(2) sites for both samples. The Cu(2)-located Fe is in the ferric high spin state, presented AF order with a transition temperature T_N strongly dependent on the oxygen content. The iron located at the Cu(1) site is in the ferric $S = \frac{3}{2}$ state and presents magnetically split spectra only at low temperatures for both samples.

ACKNOWLEDGMENTS

Partial support for this work was provided by the EC through the B/E-CT91-472 project.

[1] J. M. Tarascon, P. Bardoux, P. F. Miceli, L. H. Greene, G. W. Hull, M. Eibschutz, and S. A. Sunshine, Phys. Rev. B **37**, 7458 (1988).
[2] J. Jing, J. Bieg, H. Engelmann, Y. Hsia, U. Gomser, P. Gutlich, and R. Jacobi, Solid State Commun. **66**, 727 (1988).
[3] Y. Xu, M. Suenaga, J. Tafto, R. L. Sabatini, A. R. Moodenbaugh, and P. Zolliker, Phys. Rev. B **39**, 6667 (1989).
[4] A. M. Balagurov, G. M. Mironova, A. Pajaczkowska, and H. Szymczak, Physica C **158**, 265 (1989).
[5] Z. Q. Qiu, Y. W. Du. H. Tang, J. C. Walker, J. S. Morgan, and W. A. Byrden, J. Appl. Phys. **64**, 5947 (1989).
[6] G. Kallias, V. Psycharis, D. Niarchos, and M. Pissas, Physica C **174**, 316 (1991).
[7] R. S. Howland, T. H. Geballe, S. S. Ledermann, A. Fischer-Colbrie, M. Scott, J. M. Tarascon, and P. Bardoux, Phys. Rev. B **39**, 9017 (1989).
[8] Z. Zhou, M. Raudsepp, Q. A. Pankhurst, A. H. Morrish, Y. L. Luo, and I. Maartense, Phys. Rev. B **36**, 7230 (1987).
[9] M. Eibschutz, M. E. Lines, J. M. Tarascon, and P. Bardoux, Phys. Rev. B **38**, 2896 (1988).
[10] M. Eibschutz, M. E. Lines, and J. M. Tarascon, Phys. Rev. B **38**, 8858 (1988).
[11] I. Nowik, M. Kowitt, I. Felner, and E. R. Bauminger, Phys. Rev. B **38**, 6677 (1988); D. Hechel, I. Nowik, E. R. Bauminger, and I. Felner, *ibid.* **42**, 2166 (1990).
[12] A. Simopoulos and D. Niarchos, Phys. Rev. B **38**, 8931 (1988).
[13] L. Bottyan, B. Molnar, D. L. Nagy, I. S. Szucs, J. Toth, J. Dengler, G. Ritter, and J. Schober, Phys. Rev. B **38**, 11 373 (1988).
[14] C. W. Kimball, J. L. Matykiewicz, H. Lee, J. Giapintzakis, A. E. Dwight, B. D. Dunlap, J. D. Jorgensen, B. W. Veal, and F. Y. Fradin, Physica C **156**, 547 (1988).
[15] M. E. Lines and M. Eibschutz, Physica C **166**, 235 (1990).
[16] M. G. Smith, R. D. Taylor, and H. Oesterreicher, Phys. Rev. B **42**, 4202 (1990).
[17] I. S. Lyubutin, V. G. Terziev, E. M. Smyrnovskaya, and A. Ya. Shapiro, Physica C **169**, 361 (1990).
[18] C. Y. Yang, A. R. Moodenbaugh, Y. L. Wang, Y. Xu, S. M. Heald, D. O. Welch, M. Suenaga, D. A. Fischer, and J. E. Penner-Hahn, Phys. Rev. B **42**, 2231 (1990). C. Y. Yang, S. M. Heald, J. M. Tranquada, Youwen Xu, Y. L. Wang, A. R. Moodenbaugh, D. O. Welch, and M. Suenaga, *ibid.* **39**, 6681 (1989).
[19] R. Slater and C. Greaves, Physica C **180**, 299 (1991).
[20] H. Maeda, A. Koizmui, N. Bamba, E. Takayama-Muromachi, F. Izumi, H. Asano, K. Shimizu, H. Moriwaki, Y. Kuroda, and H. Yamazaki, Physica C **157**, 483 (1989).
[21] G. Kallias and D. Niarchos, Supercond. Sci. Technol. **5**, 56 (1992).
[22] R. J. Cava, A. H. Hewat, E. A. Hewat, B. Batlogg, M. Marezio, K. M. Rabe, J. J. Krajewski, W. F. Peck, Jr., and L. W. Rupp, Jr., Physica C **165**, 419 (1990).
[23] J. D. Jorgensen, B. W. Veal, A. P. Paulikas, L. J. Nowicki, G. W. Crabtree, H. Claus, and W. K. Kwok, Phys. Rev. B **41**, 1863 (1990).
[24] F. Menil, J. Phys. Chem. Solids **46**, 763 (1985).
[25] J. M. Tranquada, D. E. Cox, W. Kunnmann, H. Mouden, G. Shirane, M. Suenaga, P. Zolliker, D. Vankin, M. S. Alvarez, A. Jacobson, and D. C. Johnston, Phys. Rev. Lett. **60**, 156 (1988). J. M. Tranquada *et al.*, Phys. Rev. B **38**, 2477 (1988).
[26] J. S. Kim, J. Y. Lee, J. S. Swinnea, H. Steinfink, W. M. Reiff, P. Lightfoot, S. Pei, and J. D. Jorgensen, J. Solid State Chem. **90**, 331 (1990).
[27] M. Pissas, C. Mitros, G. Kallias, V. Psycharis, A. Simopoulos, A. Kostikas, and D. Niarchos Physica C **192**, 35 (1992).
[28] I. Mirebeau, C. Bellouard, M. Hennion, G. Jehanno, V. Caignaert, A. J. Dianoux, T. E. Phillips, and K. Moorjani, Physica C **184**, 299 (1991).
[29] J. M. Tranquada, G. Shirane, B. Keimer, S. Shamoto, and M. Sato, Phys. Rev. **40**, 4503 (1989), and references therein.
[30] A. Aharony, B. Birgeneau, A. Coniglio, M. A. Kastner, and H. E. Stanley, Phys. Rev. Lett. **60**, 1330 (1988).